

INVESTIGATION ON NON-CONVENTIONAL PMD CONTROL

Aly M. El-Iraki and M. Hanafi

Department of Marine Engineering and Naval Architecture, Faculty of Engineering,
Alexandria University, Alexandria, Egypt.

AbSTRACT

Behavior of traditional proportional plus integral plus derivative controller for continuous systems is investigated versus, that of the non-conventional algorithm of analog proportional minus delay control. Main gains of both techniques are optimized too according to the integral square of the errors performance index. The field of application is the speed regulation of marine Diesel engines. Results attained are discussed with those previously obtained with the adoption of either optimal regulator or optimized gain pseudo derivative feedback technique.

NOMENCLATURE

A(S)	Denominator of error signal in Laplace domain	\bar{K}	governor (N/cm)
\bar{A}	Reduced constant of the marine Diesel engine	ℓ	$= K/y_o$ (1/ r.p.m)
a, b	Lever arms (cm)	M	Mass of each flyball (Kg)
a_1, b_1	Arms of the walking beam (cm)	N	Numerator of J_4
B(S)	Numerator of error signal in Laplace domain	n	Revolutions per minute of Diesel engine (r.p.m)
C_2	$\partial Z / \partial n_{in} i$ (cm/r.p.m)	n_i	Nominal r.p.m. of Diesel engine (r.p.m)
C_3	$= C_f \cdot C_r \cdot M \cdot n_i^2$ (N/cm)	n_{in}	Command signal (r.p.m)
C_4	$= 2 C_f \cdot C_r \cdot M \cdot R_i \cdot n_i$ (N/r.p.m)	R	Radius of rotation of flyballs (cm)
C_f	$= 2 (2\pi c_g / 60)^2$	S	Laplacian operator (s^{-1})
C_r	$= b/a$	T	Time constant of the marine Diesel engine (s)
C_g	Gear ratio between engine and speed governor	T_1, T_2	Time constant of the phase lag compensator ($T_1 < T_2$) (s)
D	Denominator of J_4	t	time (s)
e(t) or E(s)	Error signal in time or Laplace domain	V	Displacement of the pilot valve (mm)
F_c	Centrifugal force on governor (N)	u	Fuel rack position (%)
F_s	Spring force on governor (N)	W	Frequency of both input and output of the loop (rad/s)
h	Dead time of PMD element (s)	X	Displacement of the bottom spring plate (mm)
i	Either suffix indicating the operating condition or $\sqrt{-1}$	X_1, X_2, X_3	State of D.E
J_4	Integral of the square of the error performance index for third over fourth order quotient error polynomials	Y	Displacements of power piston (mm)
K	$= C_2 \cdot K_s / (K_s - C_r \cdot C_3)$ (cm/r.p.m)	Y_1, Y_2	Displacements shown in Figure (3) (mm)
K_1, K_2	Spring constants in minor feedbacks of the servomotor (N/mm)	y_o	Maximum stroke of fuel rack (cm)
K_M	Gain of PMD element (s)	Z	Displacement of upper spring plate (reference signal) (mm)
K_s	Spring constant of the centrifugal governor	α	Inclination of arm (b) w.r.t. horizontal axis (deg)
		β_1, β_2	Dashpots coefficients (N.s/mm)

$\Delta..$	= change in	
τ	Servomotor's time constant	(s)
τ_1	= β_1/k_1	(s)
τ_2	= β_2/k_2	(s)
ϕ	Phase margin	(deg)
ω	Angular speed of engine	(rad/s)
ω_1	Gain cross over frequency	(rad/s)

INTRODUCTION

The establishment of control engineering technology in what concerns the fundamental principles for the determination of conventional controllers properties and specifications to suit a regulating system for a specified plant has urged researchers to develop new techniques and control algorithms whose merits overweigh those of traditional controllers. In an earlier study [1], an investigation of the performance of optimal controllers-compromising both the error function and control energy-versus the dynamic behavior of optimized gain pseudo derivative feedback (PDF) control applied to the speed regulation of marine Diesel engine has been carried out. Since the last years of the sixth decade, increasing attention was oriented to the analysis and study of control systems with time delays (deal time) [2-6]. The interest was extended too to the investigation of intentionally imposing a delay time to the controller.

Suh and Bien [7] proposed the introduction of the proportional minus delay (PMD) control element located in the major feedback line and whose transfer

function has the form: $1 + \frac{k_M}{h} (1 - e^{-h.s})$ which physically represents a pulse function followed after a time (h) by a reduced step function.

A comparison held between the (PMD) and (PD) controllers [7] when being adopted to theoretical plants showed the advantageous effects gained with the former technique. Such merits comprise swifter response, less and earlier overshoots and quicker settling of the automatic loop.

Likewise [1], the objectives of this study is the investigation of the dynamic behavior of the automatic speed control loop of the marine Diesel engine with optimized gain (PMD) control element versus its performance with the traditional (PID) controller when optimizing its main proportional gain. Furthermore, a general assessment of the adoption of optimal controller, optimized (PDF), (PMD) or (PID) controllers may lead to beneficial trends.

Several conventional speed regulators [8-12] for

marine applications are demonstrated in Figures (1-a,b,c,d) and (2-a,b).

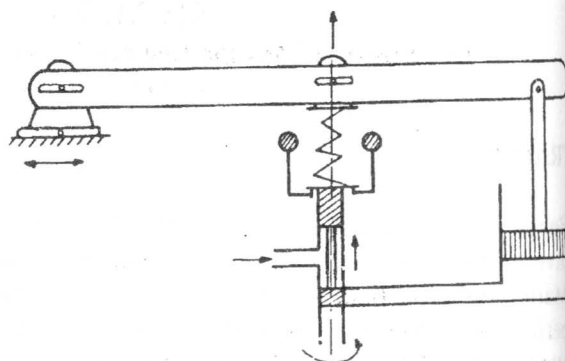


Figure 1-a. Simple governor.

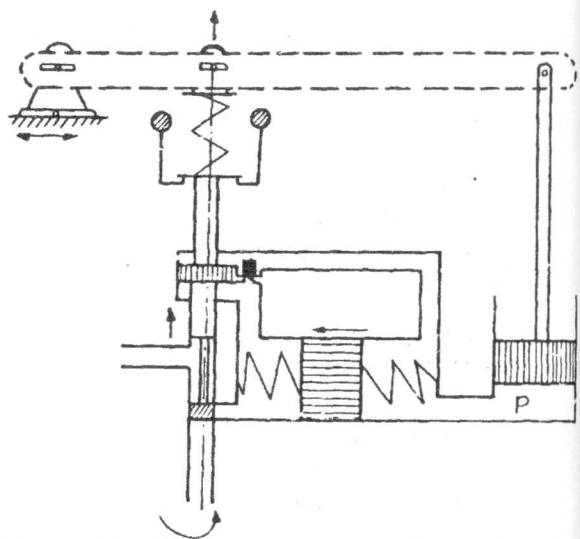


Figure 1-b. Pressure compensated governor.

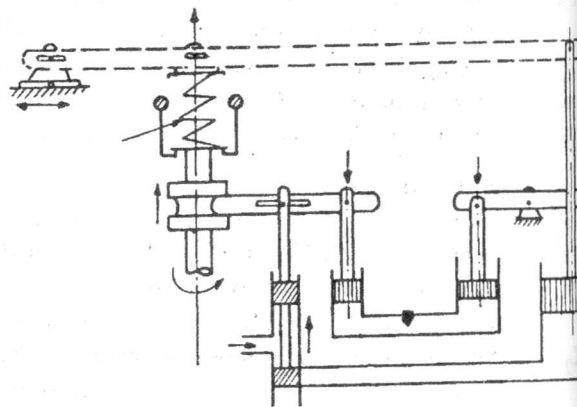


Figure 1-c. Universal governor.

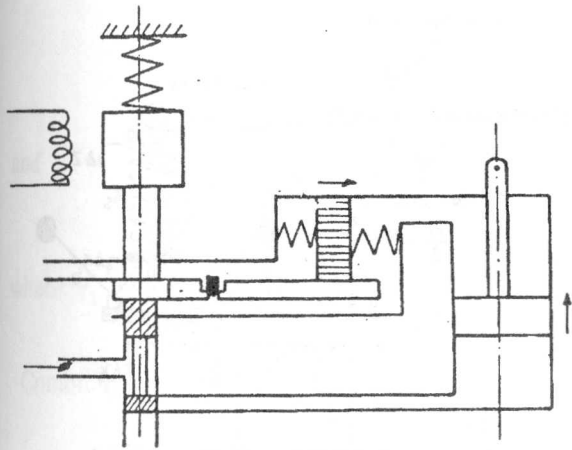


Figure 1-d. Electrical governor.

$$\begin{bmatrix} \dot{X}_1 \\ \dot{X}_2 \\ \dot{X}_3 \end{bmatrix} = \begin{bmatrix} -1.9713 & 23.75572 & -11.78886 \\ 0 & -40 & 40 \\ 0.56 & 0 & -10 \end{bmatrix} \begin{bmatrix} X_1 \\ X_2 \\ X_3 \end{bmatrix} + \begin{bmatrix} 0 \\ 0 \\ 8 \end{bmatrix} \Delta u$$

$$\text{and } \Delta n = [9.55 \quad 0 \quad 0] [X_1 \quad X_2 \quad X_3]^T \quad (1)$$

or

$$\frac{\Delta n(S)}{\Delta u(S)} = \frac{-900.668904 S + 36026.75616}{S^3 + 51.9713 S^2 + 505.1667616 S + 524.449536} \quad (2)$$

Neglecting Dead and delay times of fuel, the reduced transfer function of the plant becomes:

$$\frac{\Delta n(S)}{\Delta u(S)} = \frac{90.0668904}{S + 1.31112384} \quad (3)$$

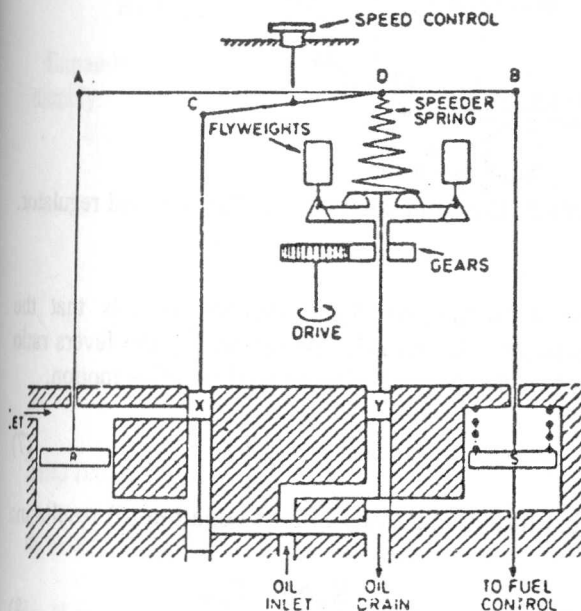


Figure 1-e. Mechanical-hydraulic controller.

MARINE DIESEL ENGINE WITH (PID) REGULATION

Mathematical analysis of speed governor and hydraulic amplifier

Dynamic simulation of the marine Diesel engine was proved to be [1]:

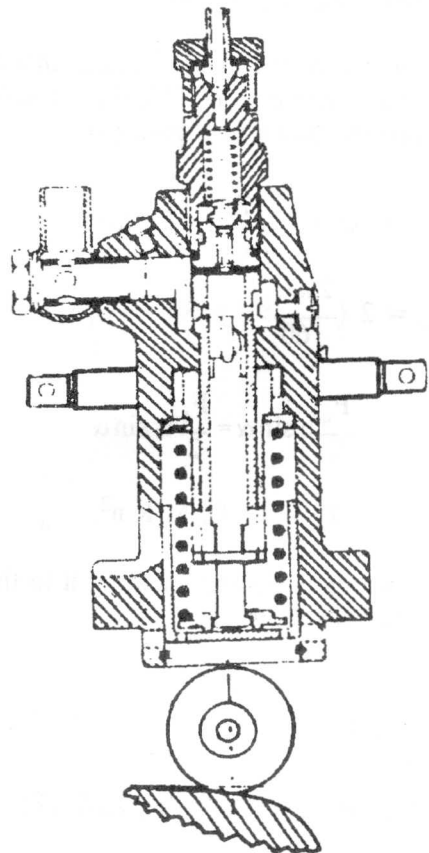


Figure 2-a. Fuel pump.

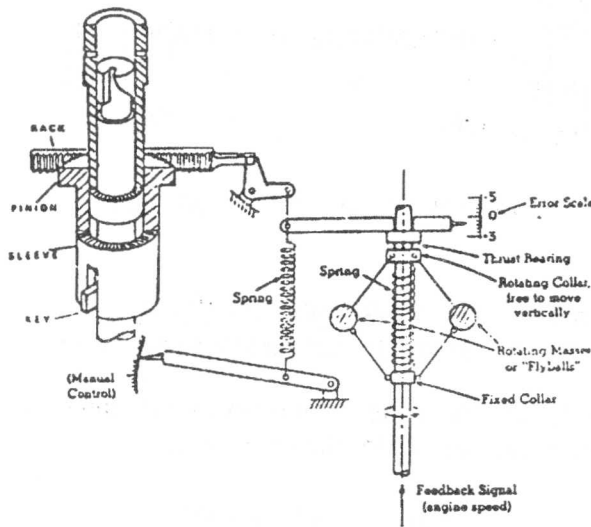


Figure 2-b. Diagrammatic representation of a self-powered Diesel engine governor.

In order to derive the mathematical model of the governor and servomotor [13,14], consider the regulating system shown in Figure (3)

$$\Delta Z = \frac{\partial Z}{\partial n_{in}} \Big|_i = C_2 \Delta n_{in} \quad (4)$$

$$F_c = 2 \left(\frac{2\pi C_g}{60} \right)^2 M R n^2 = C_f M R n^2$$

but:
$$\frac{F_c}{2} b \sin \alpha = \frac{F_s}{2} a \sin \alpha$$

or:
$$F_s = C_r C_f M R n^2 \quad (5)$$

Linearizing equation (5) and equating it to the change in spring force, it follows:

$$\Delta F_s = \frac{\partial F_s}{\partial R} \Big|_i \Delta R + \frac{\partial F_s}{\partial n} \Big|_i \Delta n = K_s (\Delta Z - \Delta X)$$

or:
$$C_3 \Delta R + C_4 \Delta n = K_s (\Delta Z - \Delta X) \quad (6)$$

where:
$$C_2 = \frac{\partial Z}{\partial n} \Big|_i, C_f = \left(2 \frac{2\pi C_g}{60} \right)^2, C_r = \frac{b}{a},$$

$$C_3 = C_f C_r M n_i^2 \quad \text{and} \quad c_4 = 2 C_f C_r R_i n_i$$

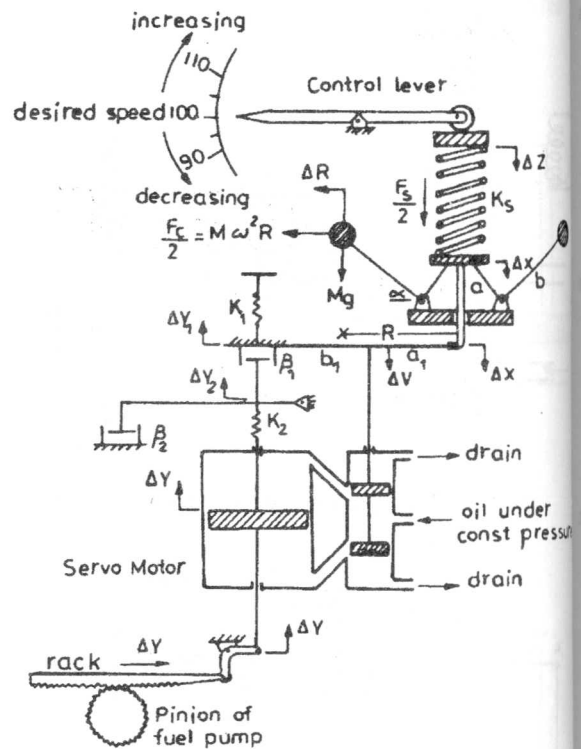


Figure 3. Dynamic analysis of (PID)₂ speed regulation

The geometry of the governor reveals that motions of ΔR and ΔX are related by the levers C_r but in the reverse direction of positive motion.

i.e.
$$\Delta R = -C_r \Delta X$$

Substituting equation (7) into equation (6) results

$$\Delta X = \frac{K_s \Delta Z - C_4 \Delta n}{K_s - C_r C_3}$$

Concerning the hydraulic amplifier the system equations describing its dynamics are:

$$\Delta Y = \frac{1}{\tau} \int_0^t \Delta V(t) dt \quad \text{or} \quad \frac{\Delta Y(S)}{\Delta V(S)} = \frac{1}{\tau \cdot S},$$

$$K_2 (\Delta Y - \Delta Y_2) = \beta_2 \Delta \dot{Y}_2 \quad \text{or} \quad \frac{\Delta Y_2(S)}{\Delta Y(S)} = \frac{1}{\tau_2 \cdot S + 1}$$

$$\beta_1 (\Delta \dot{Y}_2 - \Delta \dot{Y}_1) = K_2 \Delta Y_1 \text{ or: } \frac{\Delta Y_1(S)}{\Delta Y_2(S)} = \frac{\tau_1 \cdot S}{\tau_1 \cdot S + 1} \quad (9)$$

and

$$\Delta V(S) = \frac{b_1 \Delta X(S) - a_1 \Delta Y_1(S)}{a_1 + b_1}$$

$$\text{where: } \tau_1 = \frac{\beta_1}{K_1} \text{ and } \tau_2 = \frac{\beta_2}{K_2}$$

Combining equations (9) yields:

$$\frac{\Delta Y(S)}{\Delta X(S)} = \frac{\left(\frac{b_1}{a_1 + b_1}\right) \cdot \left(\frac{1}{\tau \cdot S}\right)}{1 + \left(\frac{1}{\tau \cdot S}\right) \left(\frac{1}{1 + \tau_2 \cdot S}\right) \left(\frac{\tau_1 \cdot S}{1 + \tau_1 \cdot S}\right) \left(\frac{a_1}{a_1 + b_1}\right)} \quad (10)$$

Expanding equation (10) gives the transfer function relating the servomotor's displacement to the error signal namely:

$$\frac{\Delta Y(S)}{e(S)} = \bar{K} \cdot b_1 \frac{(\tau_1 + \tau_2)}{\tau(a_1 + b_1) + \tau_1 a_1} * \left\{ \frac{\frac{\tau_1 \tau_2}{(\tau_1 + \tau_2)} S^2 + S + \frac{1}{(\tau_1 + \tau_2)}}{S \left[\frac{\tau \tau_1 \tau_2 (a_1 + b_1)}{\tau(a_1 + b_1) + \tau_1 a_1} \right] \cdot S^2 + \frac{\tau(\tau_1 + \tau_2)(a_1 + b_1)}{\tau(a_1 + b_1) + \tau_1 a_1} \cdot S + 1} \right\} \quad (11)$$

Data introduced

$$n_i = 99.8 \text{ r.p.m, } R_i = 0.1 \text{ m, } C_g = 1, C_r = 2,$$

$$C_f = 0.0219, M = 1.14215 \text{ kg, } C_4 = 1 \text{ N/r.p.m,}$$

$$C_3 = 5, \text{ N/cm, } y_o [1] = 6 \text{ cm, } C_2 K_S = 1 \text{ N/r.p.m,}$$

$$K = \frac{C_2 K_S}{K_S - C_r C_3}, \bar{K} = \frac{k}{y_o} \text{ and}$$

the overall speed regulating systems transfer function is taken as:

$$\frac{\Delta Y(S)}{e(S)} = \frac{\bar{K} (0.25 S^2 + S + 0.025)}{S \cdot (0.04 S^2 + 0.2 S + 1)} \quad (12)$$

Where \bar{K} is the proportional gain required to be optimized by the ISE performance index for the $(PID)_2$ controller described by equations (11,12)

Equations 2,4,8 and 12 which describe the dynamics of the automatic speed control loop are pictorially displayed

in block diagram form in Figure (4-a). Nevertheless, the simplified plant expressed by equation (3) together with the controller described by equations: (4), (8) and (12) are illustrated in Figure (4-b).

Determination of the optimized gain for the $(PID)_2$ controller

The error signal in Laplace domain for unit step input can be deduced from Figure (4-b) as:

$$e(S) = \frac{0.04S^3 + 0.259445S^2 + 1.262225S + 1.31112384}{0.04S^4 + 0.252445S^3 + (1.262225 + 22.516723\bar{K})S^2 + (1.31112384 + 90.06689\bar{K})S + 2.2516723\bar{K}}$$

$$\text{i.e. } e(S) = \frac{b_3S^3 + b_2S^2 + b_1S + b_0}{a_4S^4 + a_3S^3 + a_2S^2 + a_1S + a_0} = \frac{B(S)}{A(S)}$$

To clarify that all roots of $A(S)$ are located in the left hand side of the complex plane, the first column of Routh table for the denominator of $e(S)$ is:

$$0.04, 0.25445, (1.054477 + 8.24559\bar{K}),$$

$$\left[(1.31112384 + 90.06689\bar{K}) - \frac{0.5684234\bar{K}}{(1.054477 + 8.24559\bar{K})} \right]$$

and $2.2516723\bar{K}$

Which is certainly positive for any positive value of the overall gain $\bar{K} = \frac{K}{y_0}$. Consequently, according to [15] application of ISE performance index and Parseval's theorem gives:

$$\int_0^t e^2(t) dt = \frac{1}{2\pi i} \int_{-i\infty}^{+i\infty} \frac{B(S) \cdot B(-S)}{A(S) \cdot A(-S)} = J_4 = \frac{N}{D}$$

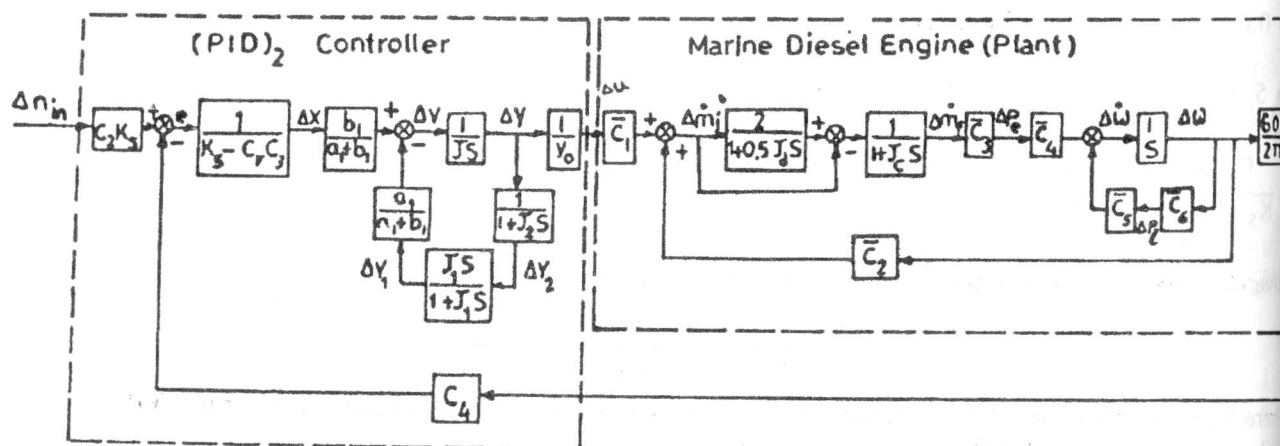


Figure 4. Automatic speed regulation system of marine Diesel engine.

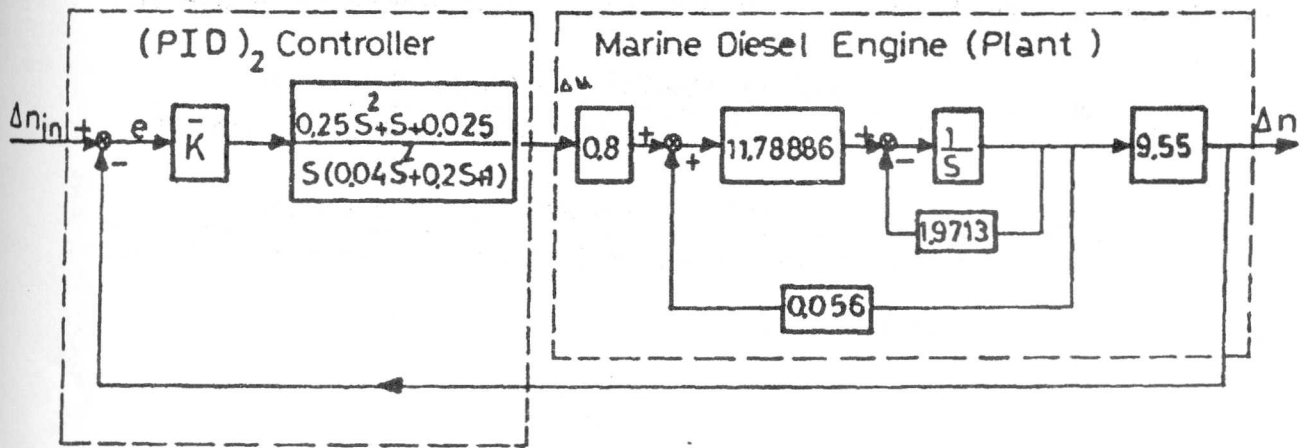


Figure 4-b. Block diagram of Figure (4-a) with selected data.

where:

$$N = b_3^2 (-a_0^2 a_3 + a_0 a_1 a_2) + a_0 a_1 a_4 (b_2^2 - 2b_1 b_3) \\ + a_0 a_3 a_4 (b_1^2 - 2b_0 b_2) + b_0^2 (-a_1 a_4^2 + a_2 a_3 a_4) \text{ and} \\ D = 2 a_0 a_4 (-a_0 a_3^2 - a_1^2 a_4 + a_1 a_2 a_3)$$

Substituting equation (13) into equations (14) and (15), J_4 is obtained as:

$$J_4 = \frac{7.306244 \bar{K}^3 + 0.211715 \bar{K}^2 + 0.165868 \bar{K} + 0.018305}{33.71433 \bar{K}^3 + 4.784688 \bar{K}^2 + 0.062871 \bar{K}} \quad (16)$$

In order to minimize $J_4 = \frac{N}{D}$ then:

$$J'_4 = \frac{D \cdot N' - N \cdot D'}{D^2} = 0 \quad (17)$$

Adopting the iterative numerical algorithm of Newton-Raphson for the solution of equation (17) we get:

$$\bar{K}_{1+1} = \bar{K}_1 - \frac{(D \cdot N' - N \cdot D')}{(D \cdot N'' - N \cdot D'')}$$

whose solution is $\bar{K} = \frac{K}{y_0} = 0.5595323966$

or $K = y_0 \bar{K} = 6 \bar{K} = 3.3571944$ and

$K_s = 10.3 \text{ N/cm}, C_2 \approx 0.1 \text{ cm/r.p.m}$

Then for unit step input, the minimum error signal and the corresponding change in speed are:

$$e(S) = \frac{0.04S^3 + 0.252445S^2 + 1.2662225S + 1.31112384}{0.04S^4 + 0.252445S^3 + 13.86106097S^2 + 51.7064666S + 1.259883597},$$

$$\Delta n(S) = \frac{12.59883597S^2 + 50.39534276S + 1.259883597}{S(0.04S^4 + 0.252445S^3 + 13.86106097S^2 + 51.7064666S + 1.259883597)}$$

and the closed loop transfer function becomes:

$$\frac{\Delta n(S)}{\Delta n_{in}(S)} = \frac{12.59883597S^2 + 50.39534276S + 1.259883597}{0.04S^4 + 0.252445S^3 + 13.86106097S^2 + 51.7064666S + 1.259883597}$$

where $e(\infty) = 0$

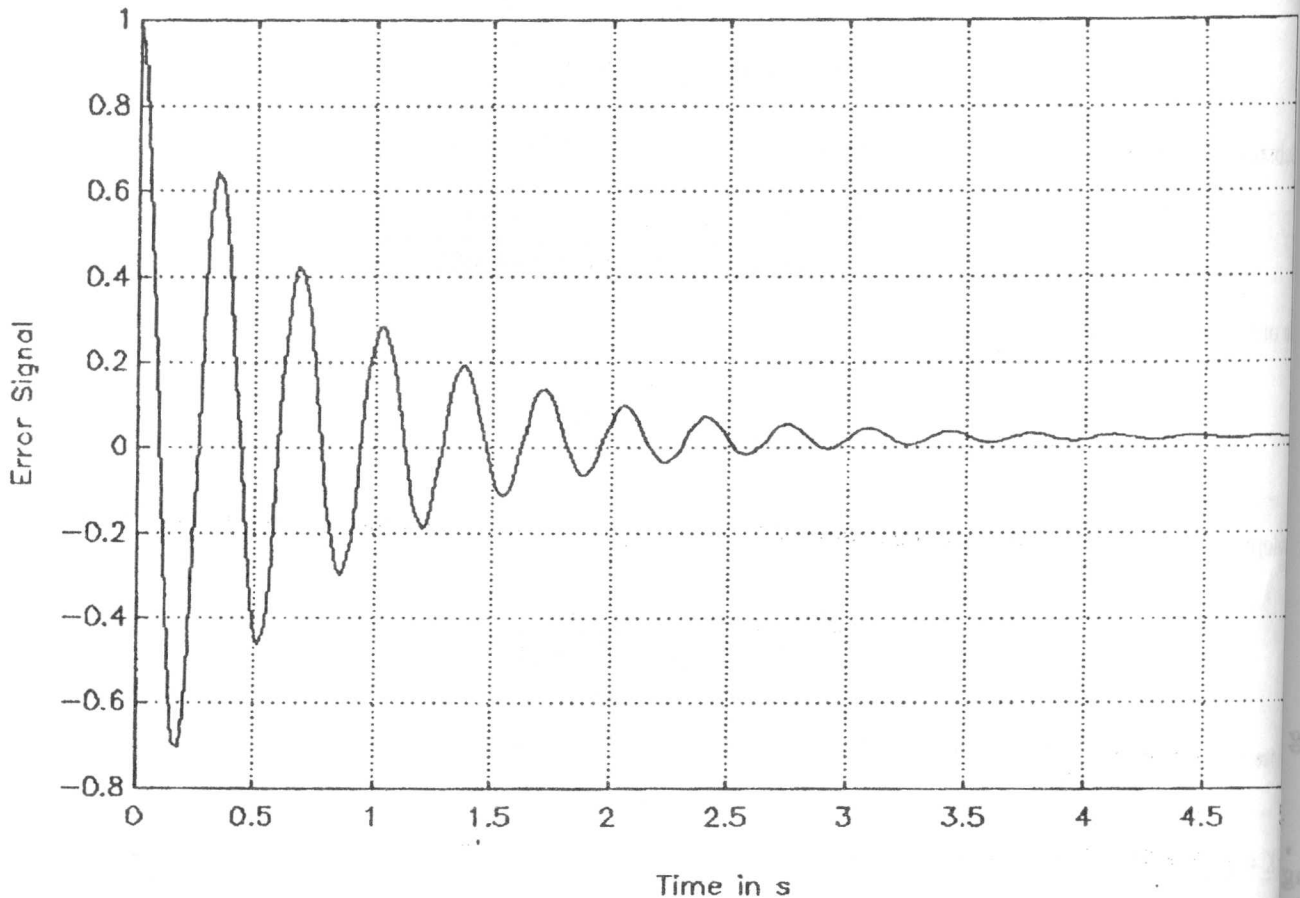


Figure 5. Transient response with PID controller.

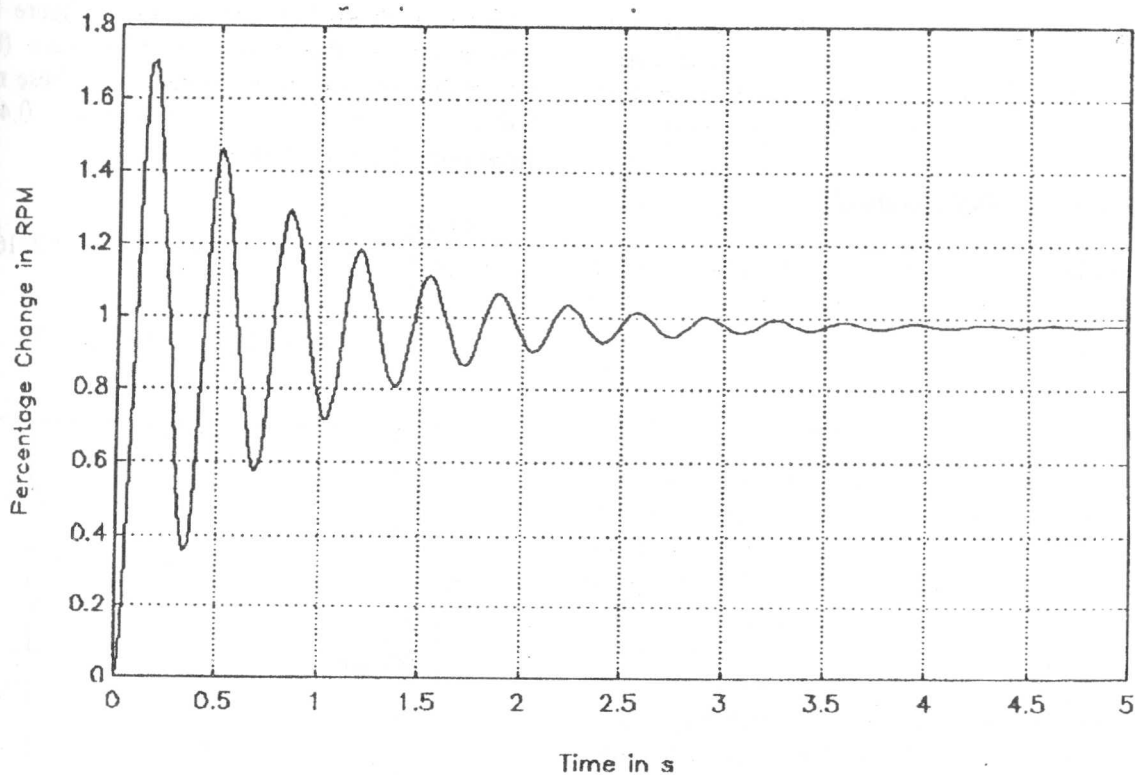


Figure 6. Speed transient response with PID controller.

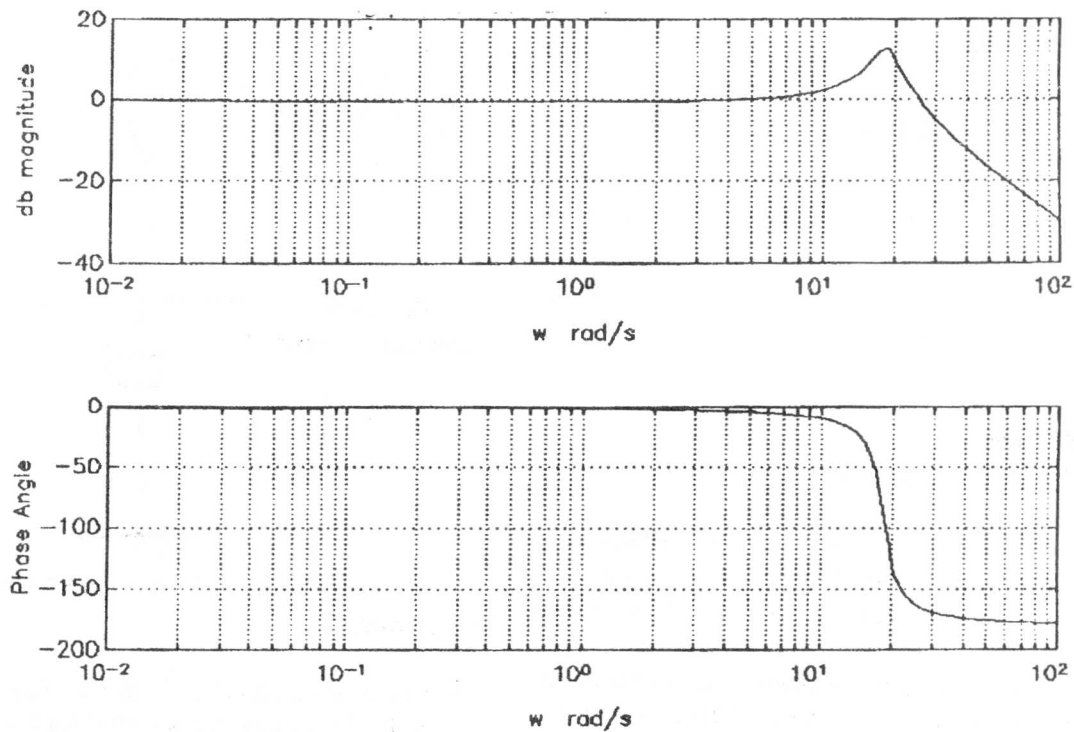


Figure 7. Optimized parameter C.L. Bode plots.

Equations (18) are plotted for the time domain response of both the error signal, the change in speed and the C.L. frequency response in Bode form and displayed in Figures (5), (6) and (7) respectively.

Optimized gain for (PMD) control

It is aimed here to investigate the behaviour of the marine Diesel engine with (PMD) control, when optimizing also both the gain K_M and the dead time h .

The forward path of the closed loop includes the D.E. cascaded to an "I_o" servomotor ($T.F. = \frac{1}{s}$) while the feedback path involves the PMD device.

Seeking for a general solution and using artificial intelligence computer package [17] for symbolic manipulation, the error signal is derived in terms of K_M and h . Pade first approximation was applied for the expansion of dead time. The error signal polynomial of (S) is evidently a quotient of third degree over fourth degree polynomials and a function of both K_M and h . Hence equation (14) and (15) still hold good for this study. Final treatment yields:

$$\frac{\partial J_4}{\partial K_M}(K_M, h) = 4.956 h^3 + 403.799 h^2 + 11.9722 h + 17.9269 = 0 \quad \text{and}$$

$$\frac{\partial J_4}{\partial h}(K_M, h) = 4.40207 h^2 + 717.076 h + 703.64375 K_M + 1024.3125 = 0 \quad (19)$$

Solution of equations (19) gives:

$$K_M = 41.4866 \text{ and } h = -81.4476, -0.0145641 \pm i 0.210237$$

Obviously such solution is refused for negative or complex dead time which physically means the instability of the control loop. A realistic solution does not exist without introducing a compensator. A generalized compensator-either phase lead or phase-lag was fed to the forward path of the loop and once again symbolic manipulations proved the existence only of unrealistic solutions with the phase lead compensators.

Lastly a phase lag compensator (Figure 8-a) was introduced to the closed loop (Figure (8-b)) and acceptable results were reached with these numerical values: $h = 0.1s$, $T_1 = 0.08s$ and $T_2 = 0.4s$ and the final optimized solution is:

$$\frac{dJ_4(K_M)}{dK_M} = 1.527 * 10^{-6} K_M^3 + 7.0216 K_M^2 - 6.36285 K_M - 2.01974 = 0$$

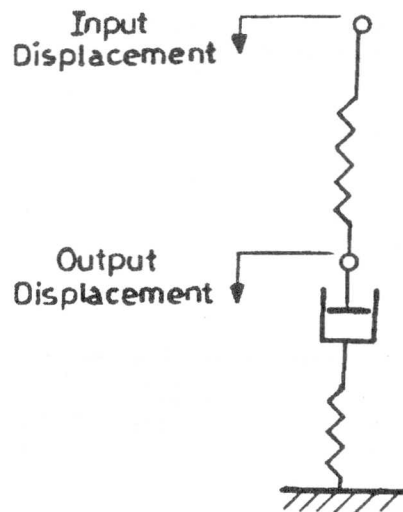
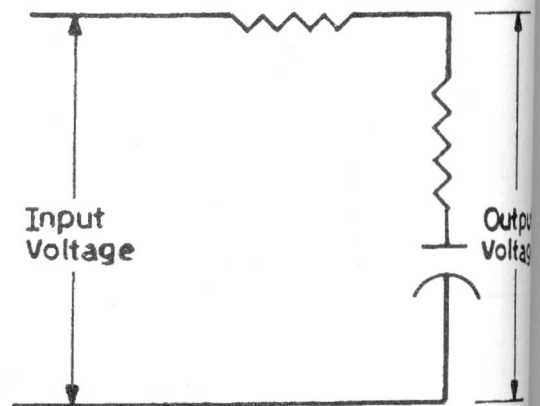


Figure 8-a. Electrical and mechanical phase compensators.

Solution of equation (20) gives: $K_M \approx 0, -0.2115518$. Excluding trivial solutions and substituting $K_M = 1.15518$ in the block diagram indicated in Figure (8-b) it follows that;

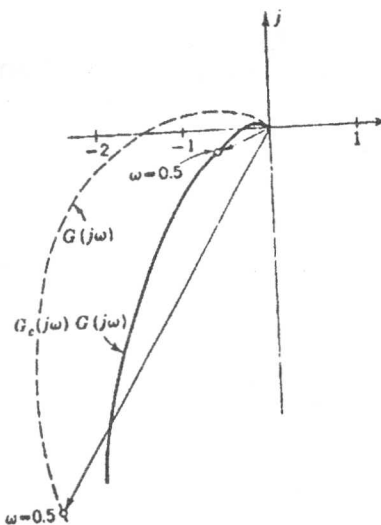
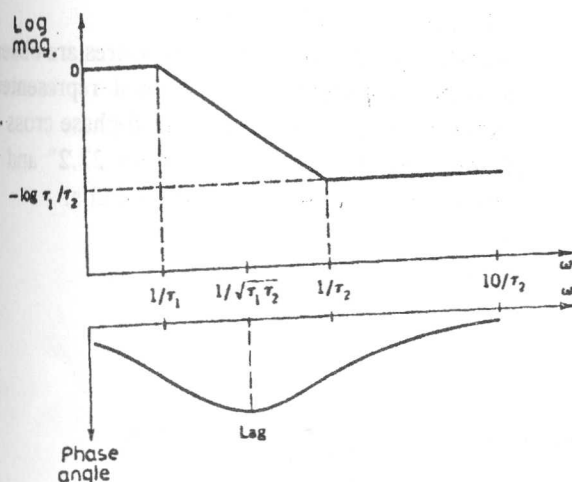


Figure (8-a)Cont. Bode plots of phase-lag compensator and its influence on reshaping polar plot.

Open loop transfer function =

$$\frac{11258.3(0.120518S^2 + 1.60647S + 1.25)}{S(3.125S^3 + 74.4097S^2 + 248.438S + 204.863)}$$

Closed loop transfer function =

$$\frac{0.0562917(2S^2 + 65S + 500)}{0.00625S^4 + 0.148819S^3 + 3.21054S^2 + 36.5822S + 28.8145}$$

and the error signal for unit step input is

$$e(S) =$$

$$\frac{20(3.125 \cdot 10^{-4}S^3 + 7.44097 \cdot 10^{-3}S^2 + 2.4838 \cdot 10^{-2}S + 2.04863 \cdot 10^{-2})}{6.25 \cdot 10^{-3}S^4 + 0.148819S^3 + 3.21054S^2 + 36.5822S + 28.1458} \quad (21)$$

where: $e(\infty) = 0$

Equations (21) are pictorially illustrated in Figures (9), (10), (11) and (12) for open loop polar plot, time domain display of error signal, change of speed and closed loop Bode plots respectively.

In addition to DERIVE [17], Packages TUTSIM and MATLAB [18,19] were made use of too.

DISCUSSION

Scanning the results obtained with (PID) controller (Figures (5), (6) and (7) in comparison with those realized with (PMD) control of the marine Diesel engine (Figures (9), (10), (11) and (12), the following remarks can be recorded:

- 1- In spite of the higher initial speed of response with the (PID) controller which can be attributed to the prompt interference of the derivative action-it renders the automatic loop oscillatory with several overshoots and excessive maximum overshoot which does not exist with the (PMD) control.
- 2- Shorter delay and rise times are noticed with the (PID) controller. In contrast, peak values and the corresponding times are not comparable since they do not exist with (PMD) control.
- 3- The incorporation of the integral property eliminates the static error with both the (PMD) and the (PID) controllers.
- 4- Settling times for 5% of the final value are nearly identical in both techniques and are close to 3.5s, 4s for (PID) and (PMD) control respectively.
- 5- Error function distribution decays more rapidly and smoothly with the (PMD) control rather than with the (PID) controller.
- 6- Resonant frequency located at $\omega = 1.8$ rad/s with the corresponding resonant peak reaching approximately 13 db characterize the closed loop frequency response with (PID) controller. In

contradiction, the closed loop frequency response with (PMD) control is distinguished by the oscillatory nature due to sinus and cosines functions produced by the dead time ($e^{-i\omega h} = \cos W - i \sin W$) without resonant frequency and peak. However, the control loop with (PID) controller seemingly

possesses a larger bandwidth if compared to loop with (PMD) control.

- 7- Satisfactory relative stability measures are observed for the loop with (PMD) control represented indefinitely large gain margin and phase cross frequency with phase margin $\phi = 22.2^\circ$ and cross over frequency. $\omega_1 = 18.8 \text{ rad/s}$.

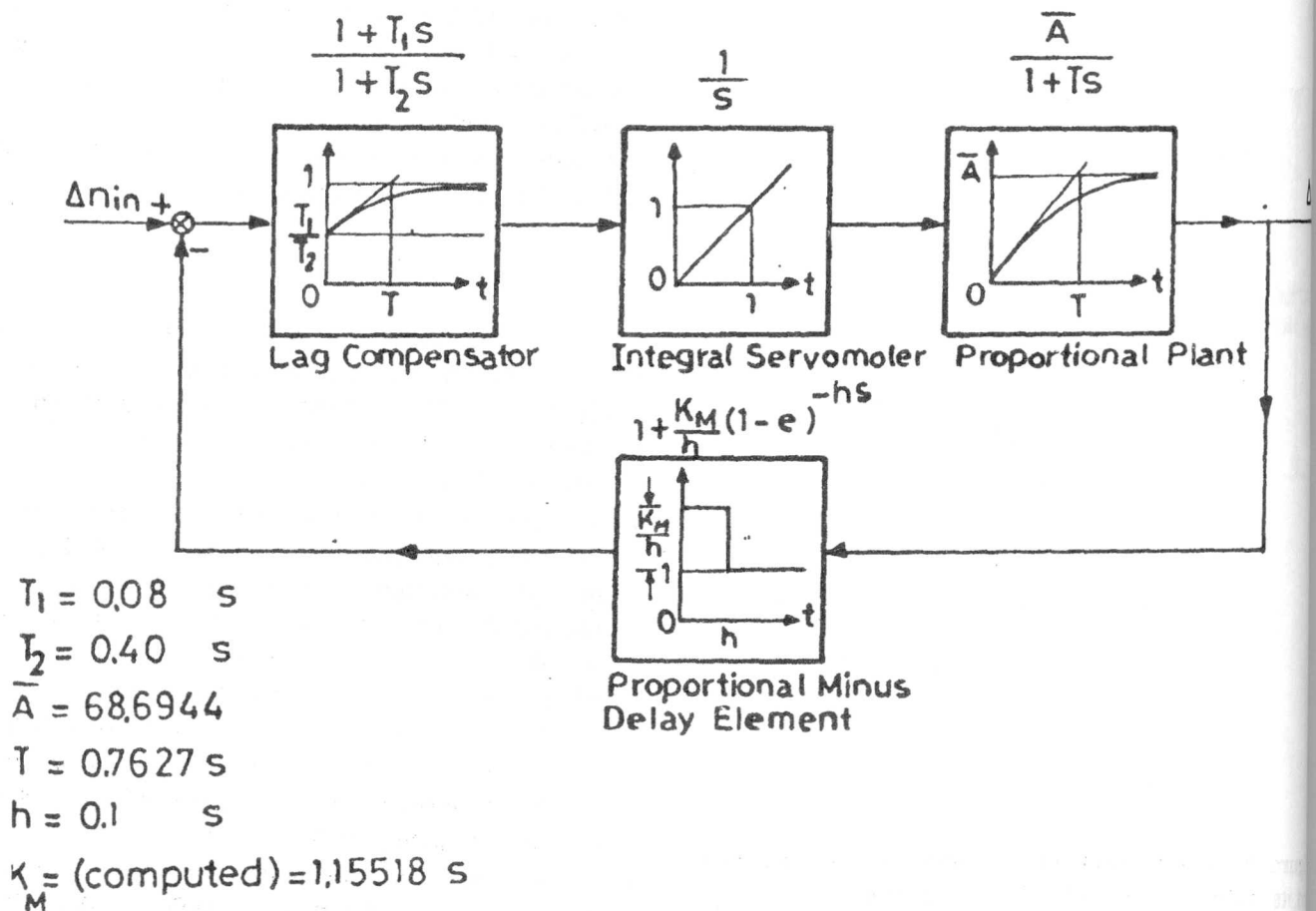


Figure 8-b. Automatic speed regulation of marine Diesel engine with PMD control.

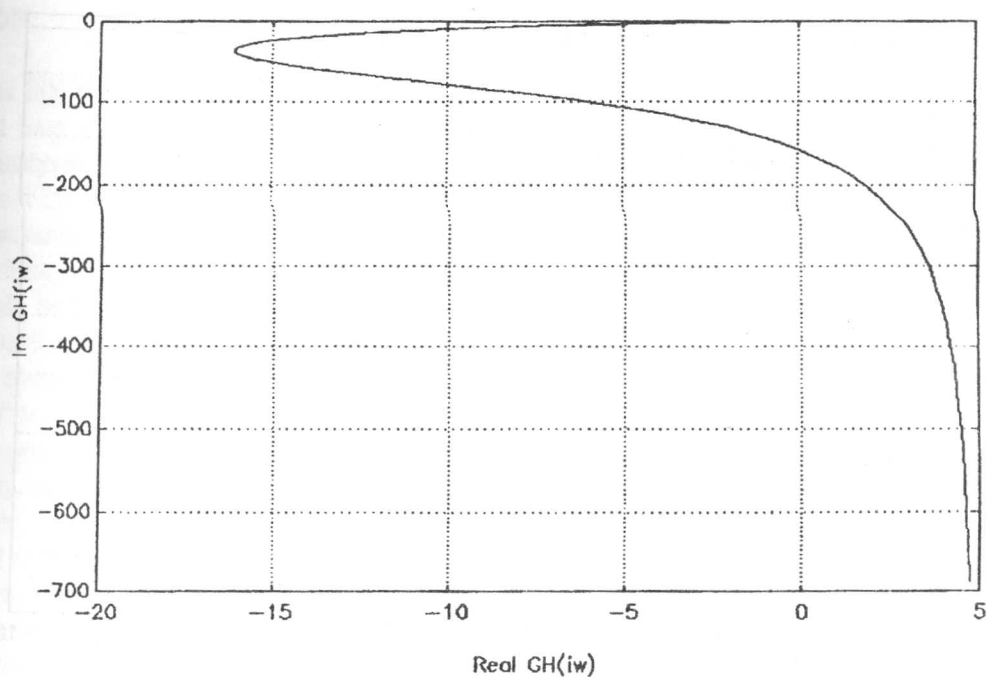


Figure 9. Polar plot with PMD.

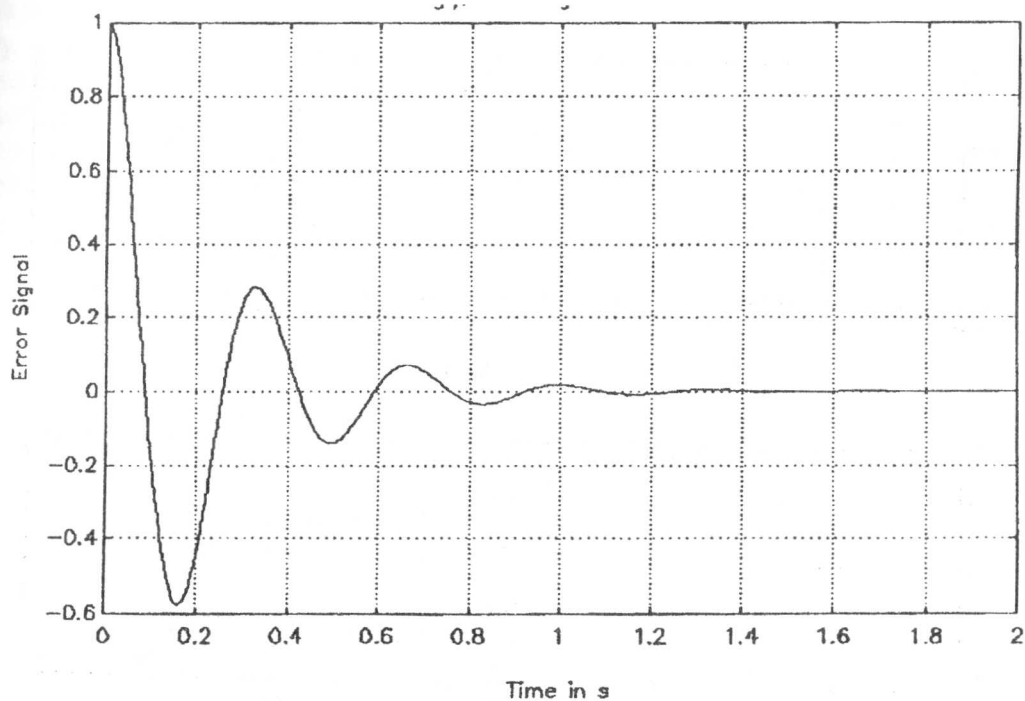


Figure 10. Error signal with PMD.

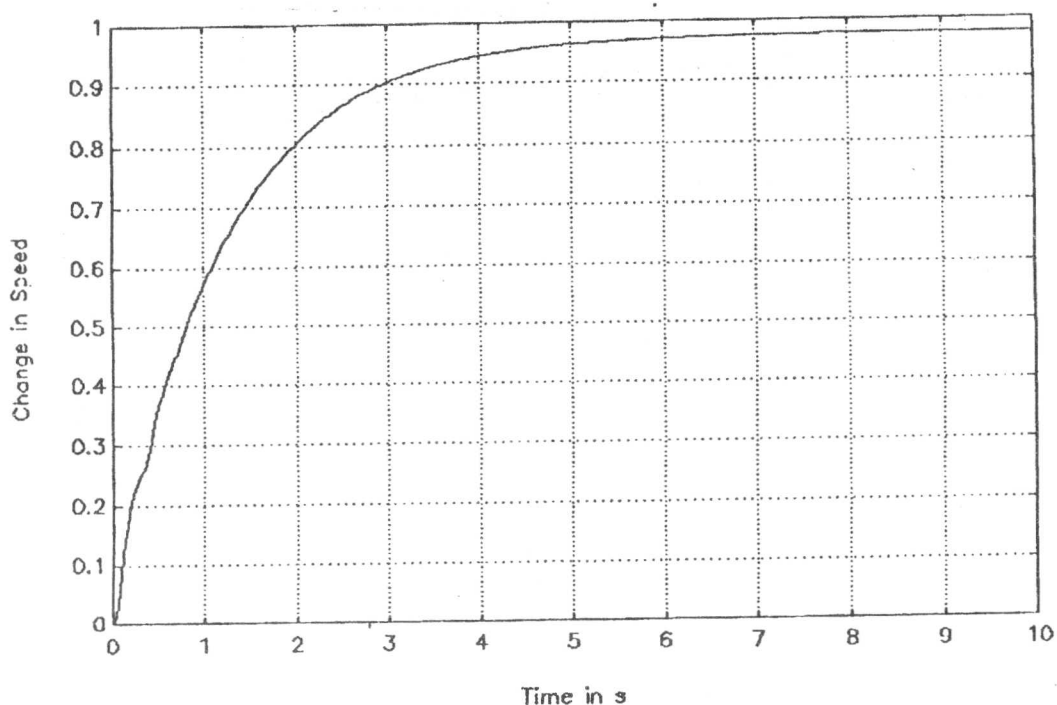


Figure 11. Optimized parameter response with PMD.

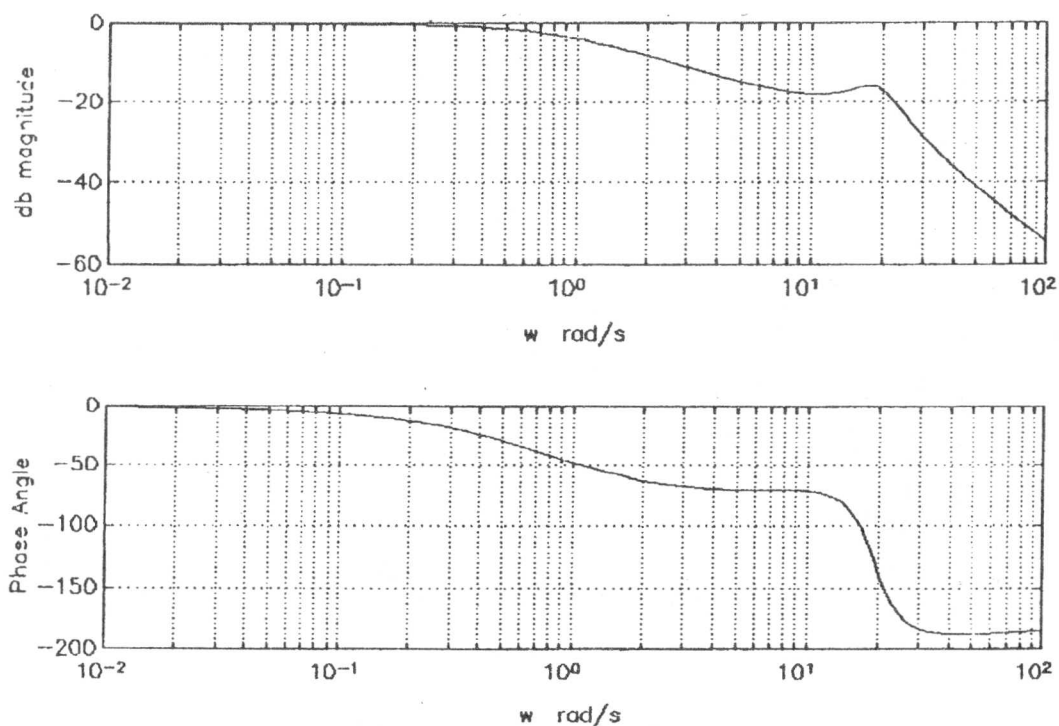


Figure 12. Bode plots with PMD.

CONCLUSION

Based on the ISE performance index, the automatic speed control loop of a marine Diesel engine was individually analyzed with both (PID) controller and (PMD) feedback control. (PMD) control proves to be undoubtedly advantageous over the (PID) controller in both time and frequency domains. Nevertheless, careful attention should be paid in regards to the encountered problem of stabilizing the closed loop compromising the (PMD) element by introducing compensating techniques. With reference to [1], it can be concluded that the linear proportional quadratic optimal regulator obtained from the solution of the reduced matrix Riccati equation involves the best performance with the marine Diesel engine, regardless of the problems of instrumentation, and state estimator's construction with the associated stability difficulties.

Next to the optimal regulator, merits of the optimized proportional minus delay (PMD) control overweigh those of the optimized pseudo derivative feedback (PDF) control, which in turn, exceed advantages attained with the optimized (PID) controller.

Apparently, other modern trends in control algorithms such as adjustable frequency controllers and non-symmetrical analog or digital controllers-where their interference is more speedy in closure rather than in admittance direction-still need thorough studies and investigations.

REFERENCE

- [1] Hanafi, M. and El-Iraki, A., *Optimized parameter versus Optimal Controllers for Marine Diesel Engines*. AEJ, July 1994.
- [2] Kleinman, D., *Optimal Control of Linear Systems with Time Delay and Observation Noise*, IEEE Trans. on Aut. Cont., Oct. 1969.
- [3] Ladde, G., *Time Lag Versus Stability*, IEEE Trans. on Aut. Cont., vol. AC-23, No. 1, febr. 1978.
- [4] Kazumasa, H. and Yoshiaki, S., *Stability of a System with Variable Time Delay*, IEEE Trans. on Aut. Cont., vol. AC-25, No.3, June 1980.
- [5] Watanabe, K. and Ito, M., *A Process Model Control for Linear Systems with Delay*. IEEE Trans. on Aut. Cont., vol. AC-25, No. 6 Dec. 1981.
- [6] Suh, and Bien, Z., *A Root Locus Technique for Linear Systems with Delay*, IEEE Trans. on Aut. cont., vol. AC-26, No. 1, Febr. 1982.
- [7] Suh, H. and Bien, Z., *Use of Time Delay Actions in the Controller Design*. IEEE Trans. on Aut. Cont, vol. AC-25, No. 3, June 1980.
- [8] _____, *The Control of Prime Mover Speed-Mathematical Analysis*. Woodward Governor Company, U.S.A., Bulletin no. 25031.
- [9] Garvey, D., *Analytic Representation of Mechanical, Hydraulic and Electro-Hydraulic Governors*, Woodward Governor Company, U.S.A. PMCC 74-14A.
- [10] Garvey, D., *Feedback Control Systems Analysis*, Woodward Governor Company, U.S.A., PMCC 74-14B.
- [11] Long, L., *Governing Systems*, Woodward Governor Company, U.S.A. PMCC 74-2.
- [12] Knak, Christen, *Diesel Motor Ships Engines and Machinery*, vol. 1&2, Marine Management Ltd, London, 1990.
- [13] Raven, F., *Automatic Control Engineering*, 3rd ed., Mc Graw-Hill, Inc. New York, 1978.
- [14] Engja, H., *Control System for Diesel Engines*, Fifth Wegemt Graduate School, Advanced Ship Power Plant Design and Operation, Paper B2, U.K. 1981.
- [15] Jury, E., *A Note on the Evaluation of the Total Square Integral*. IEEE Trans.. on Aut. Cont., vol. AC-10, No. 1, Jan. 1965, pp 110-111.
- [16] Jury, E. and Dewey, A., *A General Formulation of the Total Square Integral for Continuous Systems*, IEEE Trans. on Aut. Cont., vol. AC-10, No. 1, Jan., 1965, pp 119-120.
- [17] _____ *DERIVE a Mathematical Assistant*, 2.08, Soft Warehouse Inc., U.S.A., 1990.
- [18] _____ *TUTSIM 6.02 , Non-Linear Simulation Package*, Meerman Automation, Netherlands, 1986.
- [19] _____ *MATLAB 3.13*, the Mathworks Inc. Stanford, U.S.A, 1987.